Acquisition, Orthorectification, and Object-based Classification of Unmanned Aerial Vehicle (UAV) Imagery for Rangeland Monitoring

Andrea S. Laliberte, Jeffrey E. Herrick, Albert Rango, and Craig Winters

Abstract

The use of unmanned aerial vehicles (UAVs) for natural resource applications has increased considerably in recent years due to their greater availability, the miniaturization of sensors, and the ability to deploy a UAV relatively quickly and repeatedly at low altitudes. We examine in this paper the potential of using a small UAV for rangeland inventory, assessment and monitoring. Imagery with a ground resolved distance of 8 cm was acquired over a 290 ha site in southwestern Idaho. We developed a semi-automated orthorectification procedure suitable for handling large numbers of small-footprint UAV images. The geometric accuracy of the orthorectified image mosaics ranged from 1.5 m to 2 m. We used object-based hierarchical image analysis to classify imagery of plots measured concurrently on the ground using standard rangeland monitoring procedures. Correlations between image- and ground-based estimates of percent cover resulted in r-squared values ranging from 0.86 to 0.98. Time estimates indicated a greater efficiency for the image-based method compared to ground measurements. The overall classification accuracies for the two image mosaics were 83 percent and 88 percent. Even under the current limitations of operating a UAV in the National Airspace, the results of this study show that UAVs can be used successfully to obtain imagery for rangeland monitoring, and that the remote sensing approach can either complement or replace some ground-based measurements. We discuss details of the UAV mission, image processing and analysis, and accuracy assessment.

Introduction

Civilian applications of unmanned aerial vehicles (UAVs) have increased considerably in recent years due to their greater availability and the miniaturization of sensors, GPS, inertial measurement units, and other hardware (Lambers *et al.*, 2007; Zhou and Zang, 2007; Patterson and Brescia, 2008; Rango *et al.*, 2008; Nagai *et al.*, 2009). The advantages of using a UAV over a piloted aircraft include lower image acquisition costs than from manned aircraft, the ability to deploy the aircraft relatively quickly and repeatedly for change detection, and the ability to fly at low altitudes (Rango *et al.*, 2006).

UAVs are well suited for rangeland remote sensing applications. Due to the remoteness and low population density of rangelands, it is easier to obtain permission to fly over those areas compared to more populated areas. Land management agencies such as the U.S. Bureau of Land Management (BLM) and the U.S. Natural Resources Conservation Service (NRCS) have a requirement to monitor and assess millions of acres of rangelands, a task that is not feasible with ground monitoring techniques alone. UAVs have the potential to reduce the number of ground-based measurements required for rangeland inventory, assessment, and monitoring by providing low-cost sub-decimeter resolution digital imagery. UAVs have been used successfully, for estimating shrub utilization (Quilter and Anderson, 2001), for mapping invasive species (Hardin and Jackson, 2005), for measuring plant biomass and nitrogen (Hunt *et al.*, 2005), for documenting water stress in crops (Berni *et al.*, 2009), and for mapping rangeland vegetation (Laliberte and Rango, 2009). UAVs also allow for a landscape-level monitoring approach that offers potential for calculating landscape metrics that reflect changes in landscape processes and dynamics more accurately than plot-scale measurements alone (Bestelmeyer *et al.*, 2006).

Despite the significant potential applications of UAVs to rangeland monitoring, and recent improvements in getting from the initial image acquisition to mapping products (Laliberte *et al.*, 2007; Laliberte and Rango, 2009), more formal tests are required for future implementation of this technology. We require a better understanding of relating ground measurements in rangelands to remotely sensed information from UAV imagery, and we need to obtain data in topographically diverse environments.

One factor that has limited testing and use of unmanned aircraft for civilian applications in the United States is that the operator has to comply with the regulations of the Federal

Andrea S. Laliberte and Craig Winters are with the Jornada Experimental Range, New Mexico State University, 2995 Knox St., Las Cruces, NM 88003 (alaliber@nmsu.edu).

Jeffrey E. Herrick and Albert Rango are with the USDA-Agricultural Research Service, Jornada Experimental Range, 2995 Knox St., Las Cruces, NM 88003.

Photogrammetric Engineering & Remote Sensing
Vol. 76, No. 6, June 2010, pp. 661–672.

0099-1112/10/7606–0661/$3.00/0

Aviation Administration (FAA) concerning UAV operations in the National Airspace (NAS). The current regulations (FAA, 2008) specify that a public operator (i.e., federal, state, or local agency) has to acquire a certificate of authorization (COA) for the UAV operation. A COA provides guidelines for operator qualifications, UAV airworthiness, UAV maintenance, flying altitudes, communication with air traffic control, visual line of sight, and observer requirements. The current FAA document outlining UAV operations under a COA is subject to continuous review and is updated as required. Unfamiliarity with the COA process may also be a factor limiting the use of UAVs for rangeland assessment and monitoring.

The goal of this study was to test the feasibility of a UAV-based rangeland assessment and monitoring approach for the purpose of quantifying standard rangeland vegetation indicators for a variety of plant communities in southwestern Idaho. Planning and executing a UAV mission far from our usual UAV-operations base allowed us to complete a test that included real-world scientific and logistical constraints associated with this type of operation. Specific objectives were to compare image-based measurements with ground-based measurements in terms of accuracy, precision, and time required, and to evaluate geometric and classification accuracies of the UAV image mosaics. The focus of this paper is to describe the details of the actual UAV operation, consisting of mission planning, image acquisition, orthorectification, and mosaicking, and to report on the results of the image analysis and comparison with ground-based measurements. In addition to communicating recent advances in the development and application of these technologies, this paper should also serve as a guide for individuals and organizations that are seeking to use UAVs in the future.

Methods

Study Site

The area over which imagery was acquired was located within 3 km of the USDA Agricultural Research Service (ARS) Reynolds Creek Experimental Watershed (RCEW) headquarters at Reynolds Creek in the Owyhee Mountains of southwestern Idaho. Elevation in the image acquisition areas ranged from 1,195 m to 1,345 m. Dominant grass species at the site included Sandberg bluegrass (*Poa secunda*), squirreltail (*Elymus elymoides*), cheatgrass (*Bromus tectorum*), and dominant shrub species included big sagebrush (*Artemisia tridentate ssp. tridentata*), shortspine horsebrush (*Tetradymia spinosa*), spineless horsebrush (*Tetradymia canescens*), spiny hopsage (*Grayia spinosa*), yellow rabbitbrush (*Chrysothamnus viscidiflorus*), and silver rabbitbrush (*Chrysothamnus nauseosus*).

BAT 3 UAV and Sensors

The UAV used in the project was an MLB BAT 3 UAV (MLB Company, 2008). The BAT system consists of a fully autonomous GPS-guided UAV with a 6-foot wingspan, a catapult launcher, ground station with mission planning and flight software, and a telemetry system (Figure 1). Once launched off the catapult, the BAT acquires the first waypoint, flies the programmed flight lines, and acquires images at 75 percent forward lap and 40 percent side lap suitable for photogrammetric processing. The moving map display on the ground station shows the aircraft's location and other parameters, such as speed, altitude, and fuel level in real time. Waypoints can be changed and uploaded to the aircraft in real time.

The UAV carries two sensors: a color video camera with optical zoom capability in-flight and live video downlink to the ground station, and a Canon SD 900 ten megapixel digital camera, which is used for image acquisition. The camera acquires imagery in true color (red, green, blue (RGB), with 8-bit radiometric resolution. The size of the camera's sensor is 3,072 pixels $\times$ 2,304 pixels, with a field of view of 53.1 degrees, resulting in an individual image footprint of 213 m $\times$ 160 m, and a nominal resolution of 6 cm from an altitude of 214 m (700 feet). The onboard computer records a timestamp, GPS location, elevation, pitch, roll, and heading for each acquired image. The BAT has an endurance of two to six hours, but the current limitation is the capacity of the camera's 8-gigabyte memory card.

Project Overview

This project consisted of several tasks related to UAV operations, image processing and analysis, collection of ground-based measurement, and accuracy assessment, the latter of which included geometric accuracy of imagery, classification accuracy, and comparison of results between

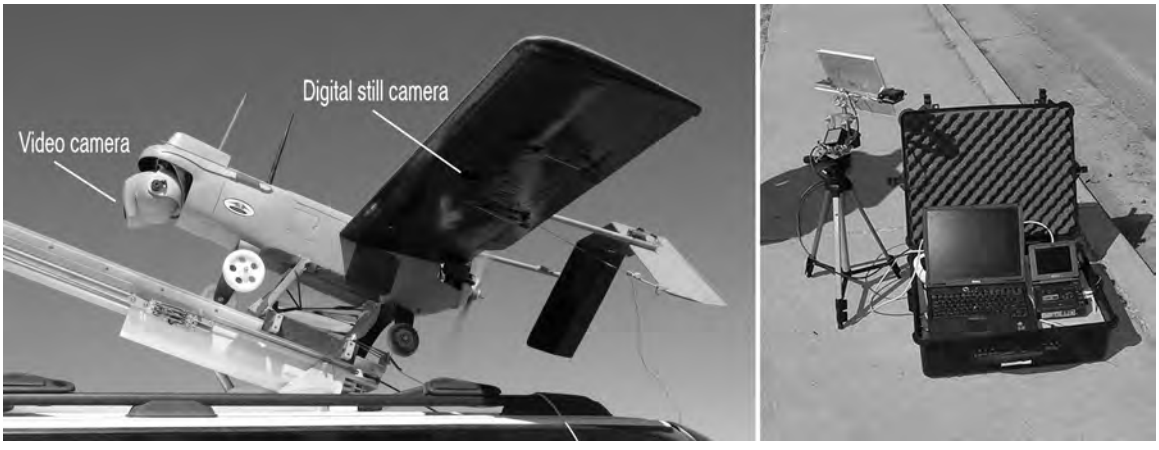

Figure 1. BAT 3 UAV on the catapult on top of the launch vehicle. The video camera is housed in a three-axis gimbal in the nose, and the digital still camera is mounted in the (a) left wing, and (b) ground station with laptop and video deck used for live video downlink, and telemetry antenna.

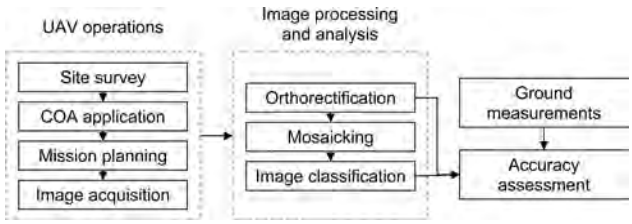

Figure 2. Flowchart of project.

image- and ground-based estimates for plot data. The tasks included (a) site survey, (b) application for a COA to the Federal Aviation Administration (FAA) to fly the UAV, (c) mission planning, (d) image acquisition, (e) image processing and analysis, (f) ground measurements, and (g) accuracy assessment (Figure 2). The individual steps are outlined in detail in the following sections.

Site Survey

The site survey included a visit by a UAV team member to the UAV flight area and inspection of the launch/landing site to assess the need for improving the landing strip. The UAV requires a relatively flat landing area of approximately 75 m × 15 m, but no paved runway is needed. GPS coordinates of the landing site were collected for mission planning, and the area was graded to create a smooth surface. While the UAV is capable of landing in vegetated areas, sites devoid of shrubs or ruts are preferred, so that the video camera in the nose of the UAV will not be damaged.

COA Application and Restrictions

We (USDA ARS) applied for the COA for this project on 13 May 2008 and received approval on 08 August 2008. The three-month time between application and approval was consistent with commonly cited approval times. The UAV operation was limited to 617 m ($\frac{1}{3}$ nautical mile) horizontal distance and 305 m (1,000 ft) vertical distance to the visual observers. Two visual observers were required to perform the "sense and avoid" function, which means that the observers are on the lookout for potential collision with other air traffic. Other requirements included that the pilot in command, ground station operator, and radio control pilot had completed private pilot ground school and passed the written test, and were in possession of a valid FAA Class 2 medical certificate, which is issued by a FAA approved physician after a physical exam (for details, see: **http://www.faa.gov/licenses_certificates/medical_certification**). The visual observers also required FAA Class 2 medical certificates.

Mission Planning

We used ArcGIS®, GoogleEarth™, as well as the UAV's ground station software for mission planning for the UAV flight. We assembled various GIS layers (digital orthoquads (DOQS), digital elevation models (DEMs), vector files of roads, etc.), and used ArcGIS® to plan the flight areas and determine flying altitudes while maintaining visual line of sight with the UAV. The current UAV ground station software cannot display elevation models, and while flights in relatively flat areas can be planned directly in the ground station software, GIS tools are required to determine visual line-of-sight from the UAV to the ground station, and to determine locations for pilots and observers in hilly terrain. We used GoogleEarth™ as a visualization tool to plan movements of pilots and observers on roads, to familiarize the crew with the landscape, and to create easily shared maps with support personnel on site. Once the coordinates for the flight areas were determined in the GIS, the information was transferred to the UAV ground station software to generate flight lines based on desired flying heights and image overlap.

Image Acquisition

On each day of image acquisition, the equipment was set up at the field location, and after UAV system checks, the UAV was launched from the catapult anchored to the top of a sport utility vehicle (Figure 1). Imagery was acquired during autonomous flight operations, and image and flight data were downloaded after landing. The UAV image acquisition flights occurred on 03–04 September 2008. The UAV team consisted of five personnel: one ground station operator, one radio control pilot, and three visual observers/support personnel. The UAV acquired imagery over three flight areas (Figure 3) in two separate flights on two separate days. The flight areas ranged in size from 70 to 130 ha, and were chosen because they were representative of the highly variable terrain typical of many rangelands, and because varying terrain affects orthorectification, mosaic creation and image analysis. Elevations in the three image acquisition areas ranged from 1,196 m to 1,340 m mean sea level (MSL), with small terrain variations in area West, intermediate variations in area North, and large variations in area East. The launch location was located at 1,235 m MSL.

The flying heights of the UAV have to be programmed relative to the launch location in meters above ground level (AGL). We held the flying heights consistent within each flight area, but had to choose different flying heights for each area due to varying terrain. The UAV acquired imagery at altitudes of 214 m above ground level (AGL) for flight area North, 275 m AGL for area East, and 183 m AGL for area West. Due to the larger terrain variations in area East, actual altitudes above the ground varied from approximately 279 m AGL in the low areas to 135 m AGL over the hill located in the upper right portion of area East. Flight areas East and West were covered by seven flight lines, and area North was covered by six flight lines.

Image Processing and Analysis

Image processing consisted of (a) orthorectification and mosaicking of UAV imagery, (b) clipping of the mosaic to the 50 m × 50 m plot areas measured on the ground, and (c) image classification. There were multiple challenges associated with orthorectification of this imagery. These challenges included the relatively small image footprints, considerable image distortion due to the use of a low-cost digital camera, difficulty in locating ground control points and in automatic tie point generation, and relatively large errors in exterior orientation parameters. We developed a semi-automated orthorectification approach suitable for handling large numbers of individual small-footprint UAV imagery without the need for manual tie points and ground control points. Input parameters include the UAV imagery, a DOQ, a DEM, exterior orientation parameters, and interior orientation parameters from a camera calibration. The process is termed PreSync and consists of initial tie-point alignment, rigid block adjustment, independent registration of each image, and subsequent realignment of tie-points, with the objective of improving the exterior orientation of the UAV imagery for further processing in photogrammetric software. Further details on the PreSync procedure can be found in Laliberte *et al.* (2008).

The six 50 m × 50 m plots that were measured on the ground were subset from the mosaics and classified

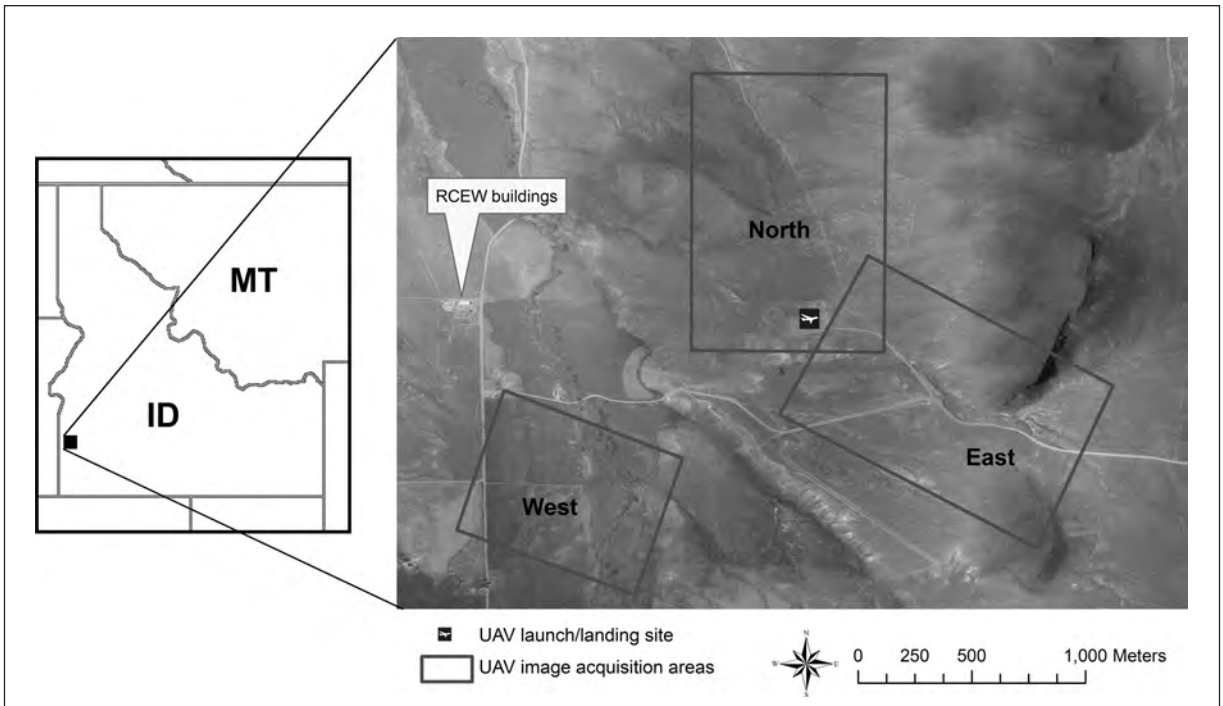

Figure 3. UAV image acquisition areas (North, East, West) near Reynolds Creek Experimental Watershed (RCEW) buildings at Reynolds Creek, Idaho (longitude 116°44'10" , latitude 43°12'18").

individually for comparison with the ground measurements. We used Definiens Developer 7.0 (Definiens, 2007), an object-based image analysis (OBIA) program, for image classification. OBIA is more suitable than pixel-based classification for high and very high resolution imagery (Hodgson *et al.*, 2003; Laliberte *et al.*, 2004; Yu et *al.*, 2006), and OBIA has been used successfully for analysis of UAV imagery (Laliberte and Rango, 2008 and 2009). With OBIA, an image is segmented into homogenous areas, followed by classification of the image segments. Segmentation is based on the three parameters scale, color (spectral information), and shape. Color and shape are weighted from 0 to 1, and within the shape parameter, smoothness, and compactness are also weighted from 0 to 1. All parameters are unit-less, and the scale parameter controls the relative size of the image segments.

The image was segmented at three scale parameters: 5, 10 (using a spectral difference segmentation), and 50. The spectral difference segmentation creates larger image objects for adjacent image objects with similar spectral responses (such as large bare areas), while maintaining small objects within (such as shrubs). The final classification was performed at scale 50. Color/shape and smoothness/compactness settings were 0.9/0.1 and 0.5/0.5, respectively. The segmentation scales and parameters were chosen based on expert judgment and visual interpretation of the results.

In addition to the six plots, we also segmented and classified the mosaics of the rangeland areas (North and East). Area West consisted of mostly private land in hayfields and was not considered for this study. The image mosaics were tiled into smaller sections, followed by segmentation and classification of the individual tiles. This approach was required because of the size and number of image objects generated by the segmentation.

Due to the limitations of spectral information for the true color bands (RGB) obtained with a relatively simple camera mounted on the UAV and the inter-correlation of those bands, imagery was transformed from the RGB space to the intensity, hue, saturation (IHS) space. In IHS space, the intensity component is separated from the color information, while the hue and saturation components relate to how humans perceive color (Jensen, 2005). This transformation has been proven useful for analysis of very high resolution UAV imagery in the past (Laliberte and Rango, 2008). A principal component analysis is another potential transformation option (Jensen, 2005), but was not investigated in this study.

We used a hierarchical classification scheme coupled with a rule-based masking approach, where the image was classified first into shadow/non-shadow areas, followed by further separation into vegetation structure groups, and then to the species level if feasible. The classification scheme was relatively generic for applicability to many rangeland communities and to other ongoing rangeland studies, and not all classes shown in the generic scheme (Figure 4) were required in every image in this study. We used rule-based classification with user-defined thresholds in the intensity band for the level 1 through level 3 classes. For the species-level classification, user-defined samples and a nearest neighbor classification algorithm were used with the following features: the means of the red, green, blue, intensity, hue and saturation bands, and the ratios of the red, green, and blue bands.

The hierarchical classification approach has several advantages: (a) classes that are more easily defined are at the top of the hierarchy, (b) the same analysis algorithm can be applied to images of different sites by changing threshold values for the classes, and (c) the method allows for comparison of results at different sites and under different conditions. For example, one might conclude that in vegetation community A, the image could be classified only to the structure group level (level 3), but in vegetation community B, a species level classification (level 4) could be obtained. This allows for developing specific goals for

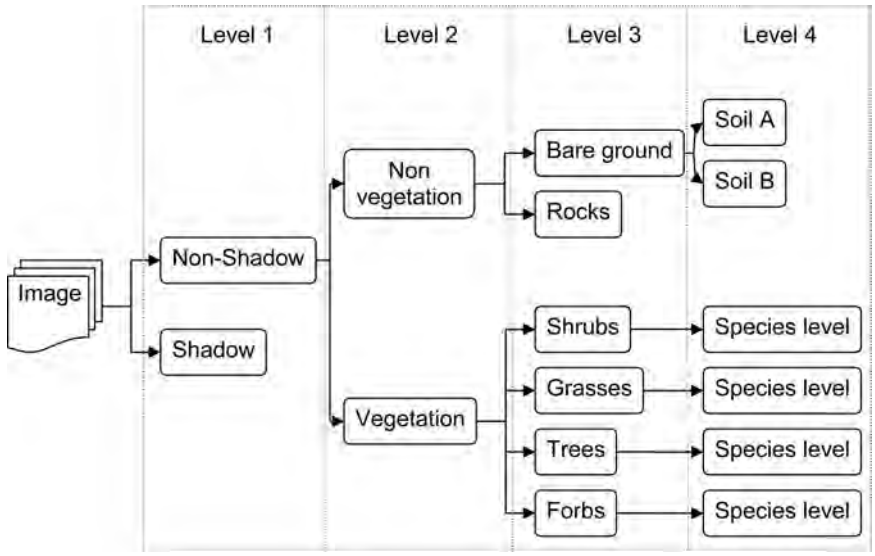

Figure 4. Hierarchical classification approach used for UAV image classification.

different vegetation communities, and can be easily incorporated into a rangeland monitoring scheme.

In Definiens, an image analysis algorithm is implemented in a process tree, which contains every action applied to the image (segmentation, classification, class creation, threshold development, etc.). The advantage of the process tree is that it can be developed on the first image, and then be applied to subsequent images with small adjustments, which was done in this study. Threshold values for separating the classes were manipulated to obtain a classification appropriate for the site. These threshold changes were required due to influences of illumination, topography, or vegetation and soil reflectance, all of which might differ between the sites. We determined suitable threshold values with visual interpretation in the "feature view" mode, which displays the segment values of a feature in gray scale and allows for visualizing changes in threshold values.

The same process tree was applied to the image mosaics with no threshold changes. Due to the large size of the image and the tiling process involved, changing and evaluating thresholds would be computer intensive and time prohibitive. We wanted to determine if the larger image mosaics could be classified with sufficient accuracy by using a process tree developed for the plot level.

Ground Measurements

Four days after the UAV flights, line-point intercept (LPI) data were collected for six 50 m × 50 m plots along six parallel 50 m transects (50 points/transect for 300 points/plot), following a standard rangeland monitoring protocol (Herrick *et al.*, 2005). We recorded all species and ground cover hits (including rock and litter) at each point, but used only the first intercept that touched vegetation or soil for the analyses, so that the results would be suitable for comparison with remotely sensed data. The species-level LPI data were grouped into the same classes used for the image classification approach (Figure 4). Three plots were located in area North, and three in area East. At the landscape level, we collected GPS data for the dominant vegetation types in each flight area to guide the accuracy assessment for the classification of the entire mosaics.

Accuracy Assessment

Accuracy assessment consisted of three parts: (a) assessing the error associated with orthorectification of the UAV imagery, (b) comparison of the ground-based and image-based estimates of vegetation cover, and (c) determination of classification errors for the image mosaics. The error associated with the orthorectification process is commonly expressed by the root mean square error (RMSE) of the aerial triangulation. Aerial triangulation refers to the process used to determine the position (*X*, *Y*, *Z*) and orientation (roll, pitch, heading) of each image in the image block, and it allows for obtaining ground coordinates for the imagery. The RMSE is a global indicator of the quality of the aerial triangulation solution and is based on the residuals of the image coordinates and the ground coordinates.

The geometric accuracy of an orthorectified mosaic is usually assessed with independent checkpoints collected on the ground. However, with such high-resolution imagery, a survey-grade GPS unit would be required for obtaining well-defined points on the ground, so that the checkpoints could fall within a pixel of the image. We did not have access to a survey-grade GPS unit, and in the absence of checkpoints, we compared the UAV mosaics with 15 cm resolution orthophotos that had been acquired with an UltraCam digital mapping camera from a piloted aircraft over the same study site on 26 August 2008, one week prior to the UAV flights. The horizontal accuracy of the UltraCam imagery was within 0.8 m of true ground.

We compared ground-based and image-based estimates of vegetation cover by determining correlation coefficients and using a paired t-test. For the accuracy assessment of the image mosaics, we used a stratified random point sampling approach with 600 points for five classes and created an error matrix to determine overall, producer's, and user's classification accuracies, and Kappa statistics (Congalton and Green, 1999). The points were evaluated by visual interpretation in conjunction with the GPS data for the dominant vegetation types.

Results

Image Acquisition

The image acquisition flights were planned to occur near solar noon to minimize shadows in the imagery. However, due to windy conditions with frequent gusts on both days, we had to move flight times to the mornings. While the BAT can be flown at wind speeds up to 25 knots, image acquisition is optimized at lower wind speeds. Imagery was acquired on Day 1 from 2:22 to 1:06 (hr:min) before solar noon, and on Day 2 from 3:35 to 2:22 before solar noon. The number of images acquired for each of the three flight areas was identical for both days, and the image acquisition times only differed by one minute for each of the flight areas. This is important for repeatability studies, where imagery has to be acquired for the same sites at different times.

Orthorectification and Mosaicking

Previously, we had only orthorectified UAV imagery originating over relatively flat areas. This imagery presented some challenges due to topography, especially in area East over the mountain. Due to the small footprint of the UAV images, large changes in elevation from image to image or within an image can result in difficulty in the image matching process. In addition, we used a rather coarse, but freely available 10 m resolution DEM in the orthorectification process. For those reasons, visible features such as roads were mismatched in some areas or did not match up as well as they would in flatter terrain. Another issue was the considerable difference in image acquisition times between the UAV imagery and the 1 m resolution DOQ used in the PreSync orthorectification process. The DOQ dated from 2004, and there were noticeable changes in area West in the hayfields near the riparian area. While there is relatively little change in rangelands from year to year, and DOQs acquired at different time periods usually work well in the PreSync procedure, changes in cultivated areas are usually larger from year to year, and in this case affected the image matching process between UAV imagery and DOQs. We observed the most problems with image matching in area West in the riparian area.

The RMSE associated with aerial triangulation is shown in Table 1. The results show that the RMSE was greatest (in cm) in the area with the most topographic relief (East). The error of the West block is mostly attributed to difficulties resulting from the image matching process. With conventional aerial photography, an RMSE of 1 pixel is desirable. This is difficult to achieve with this type of UAV imagery due to larger distortion of the imagery, greater difference between UAV image resolution and DOQ resolution, and greater differences in roll, pitch, and heading during flight. Therefore, we consider errors of 1.5 to 2 pixels from the aerial triangulation acceptable for UAV imagery acquired with low-cost cameras at this resolution.

We also compared the UAV mosaics with the UltraCam imagery by obtaining coordinates for 800 random points in the images for assessing geometric accuracies. This yielded an RMSE ranging from 1.5 m to 2 m for the three mosaics, with the highest errors for the East mosaic. Geometric accuracies of orthorectified UAV mosaics created with the PreSync algorithm in areas of little relief have been on the order of 0.5 to 1 m (Laliberte *et al.*, 2008), but we expected the accuracies to be slightly lower in areas higher relief. However, we believe that the accuracies achieved with our orthorectification approach are sufficient for rangeland monitoring purposes. Figure 5 shows the three mosaics and the six plots that were surveyed on the ground.

TABLE 1. RMSE FOR AERIAL TRIANGULATION FOR THREE FLIGHT AREAS (BLOCKS) IN IDAHO

Block	Images in block	Number of flight lines	Image resolution (cm)	RMSE (pixels/cm)
North	156	6	8	1.49/11.95
East	149	7	9	2.24/20.17
West	98	7	7	2.38/16.69

Classification of Plot Images

Image classification consisted of two steps: development of the process tree and application of the process tree to each plot image. The initial development of the process tree for the first image is usually most time consuming and strongly depends on the number of classes and complexity of the image to be analyzed. This step took approximately eight hours. Most of this time was allocated to testing and choosing appropriate segmentation scales and determining threshold levels for each feature. The second step involved creating a new project, loading the image and process tree, modifying thresholds, and selecting samples. This step took 15 to 30 minutes per image.

After the initial run of the process, which only lasted eight seconds (on a computer with 4 GB of RAM and two dual-core 2.6 GHz processors), the analyst then had to modify the threshold values for some classes if needed, and samples had to be selected if a structure group could be classified to the species level. This latter step accounted for most of the time spent on each image. Because the initial development of the process tree is most time consuming, an image analysis approach becomes more efficient as more images are analyzed for a given area.

The final classifications of the plots are shown in Plate 1. The shrub class was the only structure group that could be classified to the species level, with plots 1A, 1C, and 2C containing horsebrush, sagebrush, and rabbitbrush. We could differentiate shrubs into species, if percent cover of the species was more than 2 percent based on the ground data. Based on the LPI measurements, plot 1D contained 0.3 percent horsebrush, 2B contained 0.3 percent horsebrush, and plot 2D contained 0.3 percent rabbitbrush, while the remaining shrubs in those plots were sagebrush. Because those small shrub percentages could not be detected with image analysis, the shrub component in plots 1D, 2B, and 2D is simply shown as shrubs (in red). Similarly, we could not distinguish forbs from grasses with image analysis, and grasses and forbs were combined.

The shadow component shown in Plate 1 ranged from 2.4 percent (2D) to 6.5 percent (1D). Shadow is an added factor that needs to be addressed in the analysis of very high resolution aerial photos. In this area, the amount of shadow was largely a function of the height of the shrubs. The imagery confirmed that plot 1D contained the tallest sagebrush out of the six plots. This imagery was acquired approximately two hours before solar noon, and image acquisition closer to solar noon would decrease the shadow component.

We were able to differentiate two classes of bare ground, bare bright, and bare dark. The class bare bright indicated the brightest areas, devoid of any vegetation, with no or few small rocks, litter or biological crusts. Bare dark indicated areas that had small rocks, litter or biological crusts, but were mostly devoid of any other vegetation. The ability to clearly differentiate such areas is important for rangeland monitoring, since areas of bare ground are more susceptible to erosion, and different types of ground cover provide different levels of protection from soil detachment by raindrop impacts and overland flow.

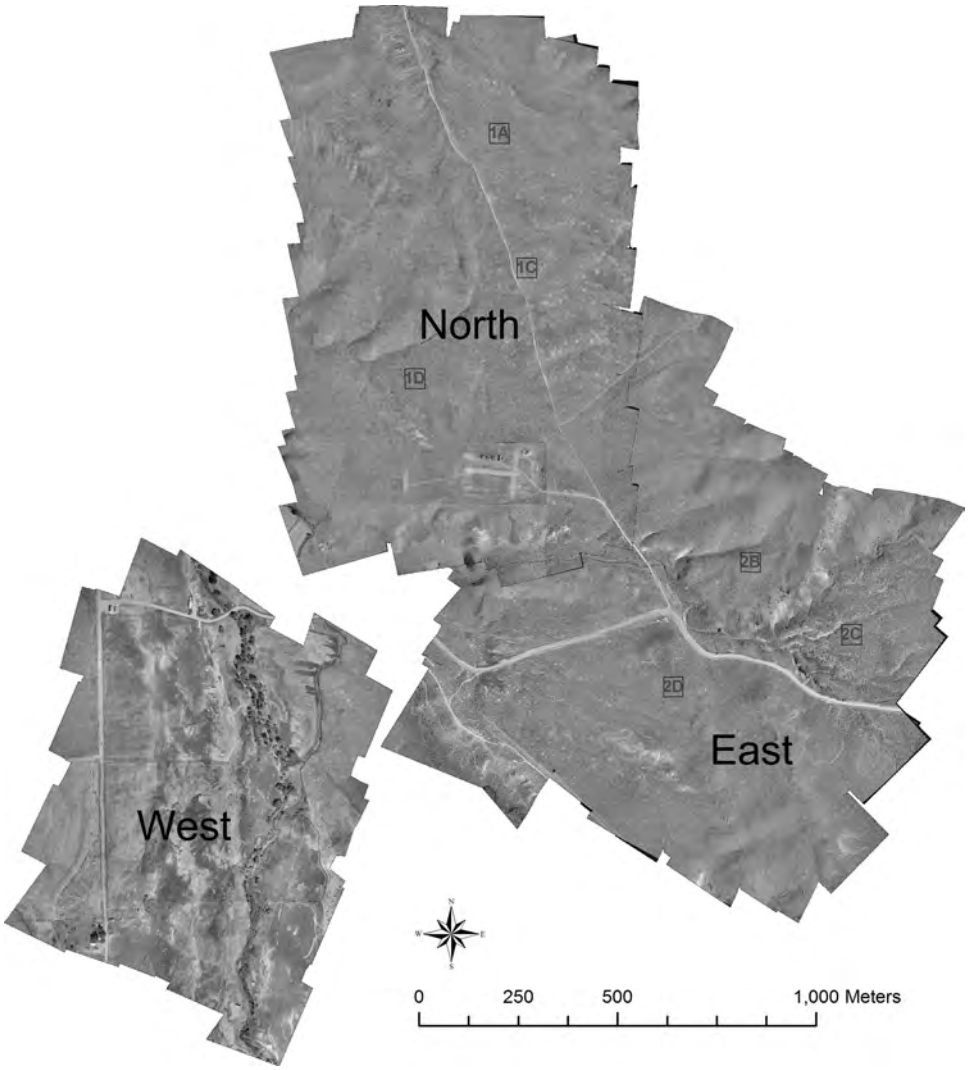

Figure 5. Three UAV image mosaics, showing the six plots that were surveyed with LPI and classified with Definiens software. The designations North, East, West refer to the same sites shown in Figure 3.

Comparison of Ground- and Image-based Measurements for Plots

The breakdown of the results for percent cover derived from LPI and image analysis for the plot data was compiled into three levels of detail: shrubs species, structure group, and bare/vegetated. We did not consider the shrub species level for correlation and regression analysis, because only three plots could be analyzed to the species level.

We obtained relatively high correlations between LPI- and image-based percent cover estimates for all four classes (bare ground, total vegetation, grass + forbs, and shrubs), with the highest values for bare ground and total vegetation (Figure 6; Table 2). Paired t-test results indicated no statistically significant differences between image- and ground-based measurements for bare ground and total vegetation, and only weak statistical differences for grass + forb (4.6 percent underestimation, p-value from paired t-test = 0.047) and shrubs (2.1 percent overestimation, p-value from paired t-test = 0.043). Coefficients of variation were higher for image-based estimates for the bare, vegetated, and grass + forbs classes, but were slightly lower than LPI-based estimates for the shrubs class (Table 2).

These results indicate very good agreement between image- and ground-based estimates of percent cover at the structure group level, demonstrating that image-based monitoring methods are viable tools to assess these parameters. In order to make reliable statements about results at the species level, a larger sample size would be required.

Time Estimates for Plot Data

We tracked the time required to obtain estimates of percent cover using ground measurements and image analysis for the plots (Table 3). Our time estimates were based on two persons obtaining LPI measurement for the six plots and deriving percent cover estimates from those data. For the image analysis approach, the time estimates included image acquisition, processing, and analysis. Image acquisition was based on a five-person UAV team for one day. The bulk of analysis time was spent on orthorectification and mosaicking of the imagery (48 hours). However, the majority of this process was computer time, and while an analyst had to be present to initiate certain modules, most of the processing was hands-off, running either overnight, or while other tasks

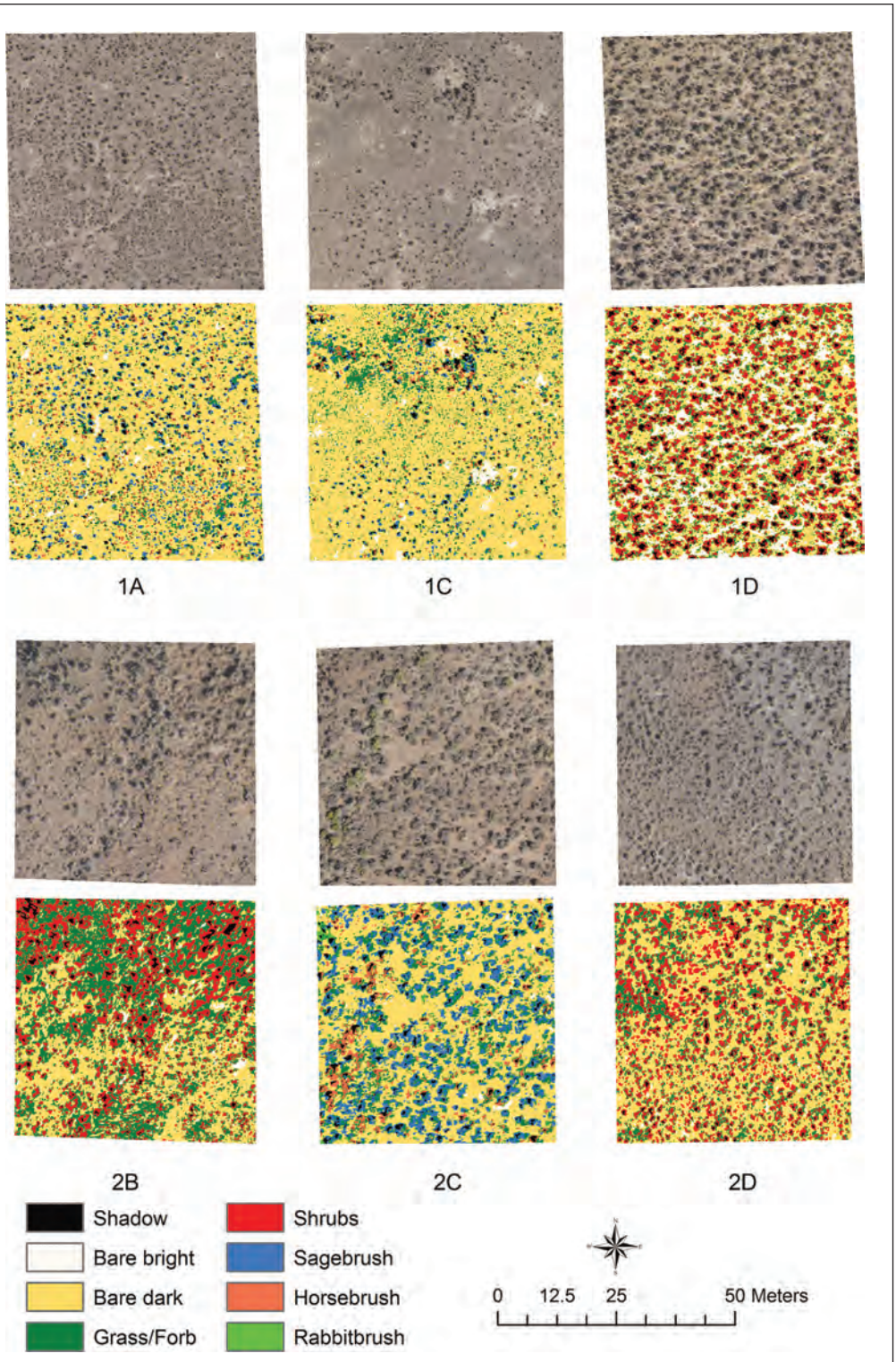

Plate 1. UAV images and image classifications of six 50 m × 50 m plots: Plots 1A, 1C, and 2C were classified to species level; plots 1D, 2B, and 2D to shrub level.

were completed. For example, the image matching process for area North took 4.5 hours (102 seconds/image), while actual operator time was estimated at around three hours. Subsequent image processing included development of the process tree and image classification.

Our time estimates showed that LPI measures required less time per plot than image analysis for only six plots. However, the advantage of the image analysis approach was that we were able to acquire UAV imagery for 290 ha in approximately two hours of flight time. This allows for

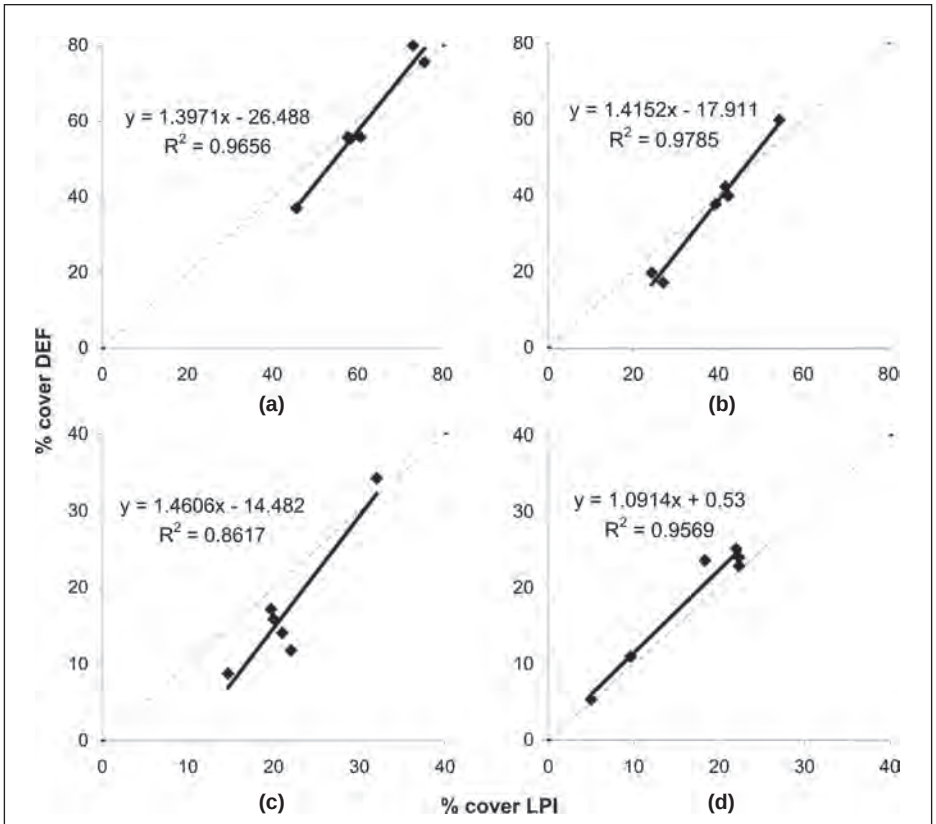

Figure 6. Correlations for percent cover estimates of six 50 m × 50 m plots using (a) line point intercept (LPI) and Definiens object-based image analysis (DEF) for (a) bare ground, (b) total vegetation, (c) grass 1 forbs, and (d) shrubs.

TABLE 2. CORRELATION COEFFICIENTS, STATISTICS FROM PAIRED T-TESTS, MEAN PERCENT COVER, AND COEFFICIENTS OF VARIATION FOR COMPARING LPI- AND IMAGE-BASED (DEF) ESTIMATES OF PERCENT COVER

	Correlation coefficient	p-value paired t-test	Mean difference	95% CI	Mean		Coefficient of variation	
					LPI	DEF	LPI	DEF
Bare ground	0.9827	0.4088	−1.93	−7.46 to 3.59	61.83	59.90	17.84	26.18
Total veg.	0.9892	0.3694	−2.07	−7.46 to 3.33	38.17	36.10	28.90	43.71
Grass+forb	0.9283	0.0469	−4.55	−9.03 to −0.08	21.56	17.00	26.49	52.85
Shrubs	0.9782	0.0434	2.05	0.09 to 4.01	16.61	18.66	45.09	44.79

TABLE 3. TIME ESTIMATES IN PERSON-HOURS FOR ACQUIRING ESTIMATES OF PERCENT COVER USING LPI MEASUREMENTS OR IMAGE ANALYSIS FOR SIX 50 M × 50 M PLOTS. LPI MEASURES ARE BASED ON TWO PEOPLE READING THE PLOTS, IMAGE ANALYSIS IS BASED ON A FIVE-PERSON UAV TEAM ACQUIRING THE IMAGERY AND ONE IMAGE ANALYST FOR PROCESSING, INCLUDING ORTHORECTIFICATION, MOSAICKING, AND CLASSIFICATION. TIME PER PLOT FOR IMAGE ANALYSIS WOULD DECLINE DRAMATICALLY WITH MORE PLOTS (SEE TEXT).

	Field time	Analysis time	Total time	Time per plot
LPI measures	72	2	74	12.33
Image analysis	40	60	100	16.67

potentially classifying a greater number of plots with little additional time compared to ground measurements. Once the imagery has been orthorectified and mosaicked, the time consuming part of the image processing steps is completed.

The time savings of UAV-based rangeland monitoring are shown in Figure 7. The image-based method has a greater efficiency, because most of the overall analysis time is used for orthorectification and mosaicking, while each additional plot only increases the overall time used by approximately 30 minutes. Each plot has to be visited and measured on the ground using the LPI method, which is more time intensive. In essence, the more plots on a mosaic are measured with image analysis, the more

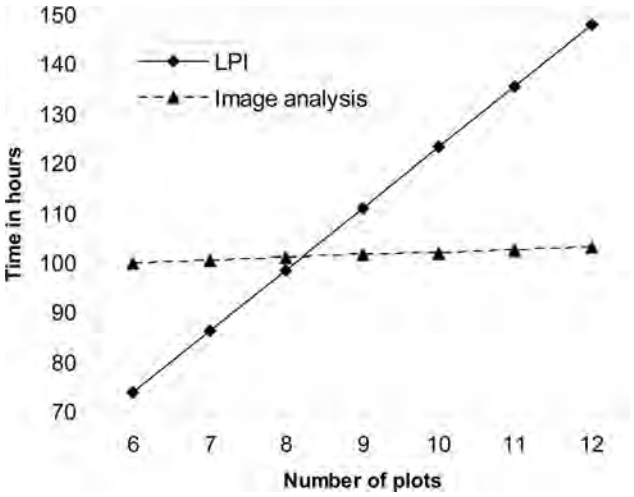

Figure 7. Time required for obtaining estimates of percent cover from ground measurements (LPI) or UAV-based image analysis versus number of plots analyzed. Results are based on surveying 50 m × 50 m plots.

efficient the image-based method becomes. In addition, the precision of the measurements for a given area is increased. Based on our time estimates for this project, the breakeven point for LPI versus image analysis is eight plots. Potential future time requirements may decrease even further based on additional automation with the orthorectification process.

Classification of Image Mosaics

We classified the image mosaics for areas North and East using the same process tree used for the plot data, with the exception that the image was first segmented into individual tiles. This approach was required to minimize the number of image objects created. The limit for Definiens is between two and five million image objects, depending on number of bands, bit depth, and complexity of image objects. Segmentation and classification of the mosaics took 10 to 12 hours, but did not require operator interaction. However, some experimentation was required initially to determine the size and number of tiles. If tiles are too large, a segmentation will exceed the maximum number of image objects. If tiles are too small, the entire process may take days to complete. We used an initial test to ensure that the image objects did not exceed the limit. In our case, 1 to 1.5 million image objects were created with tile numbers ranging from 15 to 20 tiles per mosaic. The area of the image mosaics was 65 ha for area North and 83 ha for area East; the average tile size was 3.2 ha.

Overall classification accuracies were 83 percent for area East and 88 percent for area North, with producers and users accuracies ranging from 62 to 100 percent (Table 4 and Table 5). These results are promising for this type of data and processing, given that the input to the process tree was derived only from the plot data, and not from the entire image extent. Higher accuracies are possible if more sample data for training are used (Laliberte and Rango, 2009). It also has to be considered that in this study, accuracy assessment consisted of determining class assignments for the stratified point samples based on photo interpretation of the random points on the image mosaic, because our ground sampled data did not cover the entire area. For that reason, we did not attempt to classify the mosaic imagery to the species level.

TABLE 4. ERROR MATRIX FOR CLASSIFICATION OF IMAGE MOSAIC NORTH. ROWS ARE CLASSIFICATION DATA, COLUMNS ARE REFERENCE DATA

	Shadow	Bare bright	Bare dark	Grass/ Forb	Shrubs
Shadow	21				2
Bare bright		18			
Bare dark	4	4	318	17	19
Grass/Forb			8	62	8
Shrubs	5				114
Producer's accuracy	70%	82%	98%	78%	80%
User's accuracy	91%	100%	88%	79%	96%
Overall accuracy	88%				
Kappa index	0.82				

TABLE 5. ERROR MATRIX FOR CLASSIFICATION OF IMAGE MOSAIC EAST. ROWS ARE CLASSIFICATION DATA, COLUMNS ARE REFERENCE DATA

	Shadow	Bare bright	Bare dark	Grass/ Forb	Shrubs
Shadow	18				1
Bare bright		27			
Bare dark	1	4	301	8	16
Grass/Forb			28	58	8
Shrubs	3		25	4	98
Producer's accuracy	85%	87%	85%	83%	80%
User's accuracy	95%	100%	91%	62%	75%
Overall accuracy	83%				
Kappa index	0.73				

Discussion and Conclusions

The results of this study indicate that UAV-based systems for rangeland inventory and monitoring show great promise. We were able to demonstrate the UAV's ability to revisit permanent plot locations and obtain high quality, high-resolution images. The orthorectification approach we developed does not require much operator interaction, and the orthorectified image mosaics have sufficient accuracy for rangeland monitoring purposes. There is increasing interest in the use of very large-scale aerial imagery for rangeland assessment and monitoring (Booth *et al.*, 2006; Blumenthal *et al.*, 2007; Sankey *et al.*, 2008), and a UAV is a flexible image acquisition tool for that purpose. Other recent developments are the use of UAV-based video data with near real-time orthorectification and mosaicking (Zhou, 2009).

Object-based image analysis using Definiens software was well suited for processing of this imagery, because the segmentation and classification algorithms could be developed on one image and transferred to all other images with relatively little adjustments. This increased the speed with which images could be processed into final thematic maps. It also allowed for consistency in the analysis from image to image. The hierarchical classification approach is suitable for applications in rangeland communities, and the results are useful for management decisions applicable to the different classification levels (i.e., vegetation/non-vegetation, structure group, or species level). We obtained very high correlations between ground-based and image-based estimates of percent cover for bare ground, total vegetation, grass + forbs, and shrubs. Shrubs could be differentiated

into species, if percent cover of the shrub species was more than 2 percent of the plot based on the LPI data.

The image analysis approach proved to be more efficient than ground-based measurements for the same plots. Due to economies of scale, once the UAV imagery was processed into orthorectified mosaics, the image analysis of additional plots would not increase the overall analysis time to a great extent. The ability to classify more plots once mosaics have been created would also allow for obtaining a more precise estimate of percent cover over a given area. If those plots had to be measured on the ground, time, and therefore costs, would increase at a greater rate. This is one of the advantages of remotely sensed information, even though the accuracy and level of detail may be less than that of ground based measurements.

We have also shown that it is possible to obtain a vegetation classification from the entire mosaic by using process trees developed for the plot level, and obtaining good overall accuracy values of 83 percent and 88 percent. These very high resolution thematic maps derived from the UAV mosaics offer a landscape level assessment of rangelands, although the overall accuracies could be improved by collecting more sample data for training at the landscape level.

Another possible application of the UAV-based approach is to analyze and classify individual UAV images without going through the orthorectification process. This would reduce the time spent on image processing, but with the disadvantage of having to work with unrectified images and an inability to overlay field plot coordinates on the imagery. However, this approach would allow for obtaining a large number of individual plot "samples" with considerably less cost than ground-based measurements.

The object-based image analysis approach discussed here is also highly applicable to aerial photography acquired with digital mapping cameras mounted in piloted aircraft. The spatial resolution achieved with these cameras is currently comparable or even higher, and imagery can be acquired in the near infrared, which is better suited for vegetation classification than using only RGB imagery. However, image acquisitions using piloted aircraft with larger digital mapping cameras are more costly and are better suited to mapping of larger areas than one would attempt with a UAV.

The main limiting factors of UAV-based operations are the costs associated with equipment, personnel, training, and the requirement for a COA application. The cost of the UAV used in this study (including aircraft, ground station, and catapult) was approximately 50,000 USD. The five-person crew required training in UAV operation and maintenance, private pilot ground school certificates and medical certificates. Given those initial input costs and the learning curve involved in operating a UAV for image acquisition, it is difficult to estimate a break-even point in terms of cost, but in many regards, the investment is similar to a manned aerial image acquisition project. At this stage, we are in the early phases of determining the viability of using UAVs for real-world applications, and costs are relatively high, which is the reason we concentrated on determining time savings over ground-based measurements.

The second limitation of operating UAVs is the requirement for a COA. A COA limits the areas of operations in terms of distance and altitude to visual flight rules; it requires the use of visual observers and the operation requires specifically trained personnel, all of which adds to the cost of the operation. The reason for these limitations is the FAA's requirement for a level of safety that is comparable to manned aircraft in terms of collision avoidance.

The ability to detect, sense, and avoid (DSA) conflicting air traffic is a requirement for UAV operations. Visual observers on the ground or in chase aircraft are commonly used, but ongoing research is investigating technologies such as on-board cameras or sound detectors, as well as ground-based radar for collision avoidance (Carnie *et al.*, 2006; Hutchings *et al.*, 2007). The first standard for an airborne sense-and-avoid system was released by the American Society for Testing and Materials (ASTM) in 2004 (Schaefer, 2004), and it has since been updated (ASTM Standard F2411, 2007). It is possible that such standards will be incorporated into future FAA requirements.

In April 2008, the FAA created the small unmanned aircraft systems aviation rulemaking committee (ARC), and on 01 April 2009, the ARC submitted their recommendations for small UAS regulatory development to the FAA. Future regulations will likely be based on those recommendations. Current FAA regulations and policies are available at the FAA website: **http://www.faa.gov/aircraft/air_cert/design_approvals/uas/reg/**.

The COA process is constantly changed and updated, and it is hoped that UAV operations will eventually be "file-and-fly" with shorter application periods, separation of UAVs by size class, and with the possibility of taking advantage of the UAV's autonomous capabilities to fly to more remote locations. However, as we demonstrated in this project, even under the current limitations, UAVs can be used successfully to obtain imagery for rangeland monitoring and assessment, and can complement ground-based measurements. UAVs may even completely replace these measurements where only relatively simple information, such as shrub cover, is required. Future plans include upgrading the digital camera to a multispectral or hyperspectral sensor which would improve the potential for mapping shrub and grass species.

Acknowledgments

Funding for this study was provided by the Bureau of Land Management as part of their National Assessment, Inventory, and Monitoring Strategy - Owyhee Uplands Pilot Project, and by the USDA Agricultural Research Service (ARS). Additional support for development of the tools and methods for image processing and analysis was provided by the USDA Natural Resources Conservation Service in support of the Conservation Effects Assessment Project. We are grateful for the collaboration and contributions of Fred Pierson, Mark Seyfried, and Adam Winstral from the USDA ARS Northwest Watershed Research Center. Michelle Mattocks and Noemi Baquera were responsible for collecting the field data, with logistical and data management support from Ericha Courtright and Justin Van Zee. Additional thanks go to the rest of the UAV team: Jim Lenz, Chris Pierce, Amalia Slaughter, David Thatcher, and Connie Maxwell.

References

ASTM Standard F2411, 2007. Standard specification for design and performance of an airborne sense-and-avoid system, URL: *http://www.astm.org*, ASTM International, West Conshohocken, Pennsylvania (last date accessed: 19 February 2010).

Berni, J.A.J., P.J. Zarco-Tejada, L. Suarez, and E. Fereres, 2009. Thermal and narrowband multispectral remote sensing for vegetation monitoring from an unmanned aerial vehicle, *IEEE Transactions on Geoscience and Remote Sensing*, 47(3):722–738.

Bestelmeyer, B.T., D.A. Trujillo, A.J. Tugel, and K.M. Havstad, 2006. A multi-scale classification of vegetation dynamics in arid lands: What is the right scale for models, monitoring, and restoration?, *Journal of Arid Environments*, 65:296–318.

Blumenthal, D., D.T. Booth, S.E. Cox, and C.E. Ferrier, 2007. Large-scale aerial images capture details of invasive plant populations, *Rangeland Ecology and Management*, 60:523–528.

Booth, D.T., S.E. Cox, and R.D. Berryman, 2006. Precision measurements from very-large scale aerial digital imagery, *Environmental Monitoring and Assessment*, 112:293–307.

Carnie, R., R. Walker, and P. Corke, 2006. Image processing algorithms for UAV "sense and avoid," *Proceedings of the 2006 IEEE International Conference on Robotics and Automation*, (IEEE), 15–19 May, Orlando, Florida, pp. 2848–2853.

Congalton, R.G., and K. Green, 1999. *Assessing the Accuracy of Remotely Sensed Data: Principles and Practices,* Lewis Publishers, Boca Raton, Florida, 137 p.

Definiens, 2007. *Definiens Developer 7.0 User Guide*, Definiens AG, Munich, Germany, 506 p.

Federal Aviation Administration (FAA), 2008. Interim Operational Approval Guidance 08-01: Unmanned Aircraft Systems Operations in the U.S. National Airspace System, URL: *http://www.faa.gov/aircraft/air_cert/design_approvals/uas/reg/media/uas_guidance08- 01.pdf*, FAA, Aviation Safety Unmanned Aircraft Program Office (last date accessed: 19 February 2010).

Hardin, P.J., and M.W. Jackson, 2005. An unmanned aerial vehicle for rangeland photography, *Rangeland Ecology and Management*, 58:439–442.

Herrick, J.E., J.W. Van Zee, K.M. Havstad, L.M. Burkett, and W.G. Whitford, 2005. *Monitoring Manual for Grassland, Shrubland and Savanna Ecosystems*, Volume I: Quick Start, and Volume II: Design, Supplementary Methods and Interpretation, USDA-ARS Jornada Experimental Range, Las Cruces, New Mexico, 236 p.

Hodgson, M.E., J.R. Jensen, J.A. Tullis, K.D. Riordan, and C.M. Archer, 2003. Synergistic use of lidar and color aerial photography for mapping urban parcel imperviousness, *Photogrammetric Engineering & Remote Sensing*, 69(9):973–980.

Hunt, E.R., M. Cavigelli, C.S.T. Daugherty, J. McMurtrey III, and C.L. Walthall, 2005. Evaluation of digital photography from model aircraft for remote sensing of crop biomass and nitrogen status, *Precision Agriculture*, 6:359–378.

Hutchings, T., S. Jeffryes, and S.J. Farmer, 2007. Architecting UAV sense & avoid systems, *Proceedings of the 2007 Conference on Autonomous Systems, Institution of Engineering and Technology,* (IEEE), 23–27 Nov, London, UK, unpaginated CD-ROM.

Jensen, J.R., 2005. *Introductory Digital Image Processing: A Remote Sensing Perspective*, Third edition, Prentice-Hall, Inc., Upper Saddle River, New Jersey, 526 p.

Laliberte, A.S., A. Rango, K.M. Havstad, J.F. Paris, R.F. Beck, R. McNeely, and A.L Gonzalez, 2004. Object-oriented image analysis for mapping shrub encroachment from 1937–2003 in southern New Mexico, *Remote Sensing of Environment*, 93:198–210.

Laliberte, A.S., A. Rango, and J.E. Herrick, 2007. Unmanned aerial vehicles for rangeland mapping and monitoring: A comparison of two systems, *Proceedings of the ASPRS 2007 Annual Convention*, 07–11 May, Tampa, Florida (American Society for Photogrammetry and Remote Sensing, Bethesda, Maryland), unpaginated CD-ROM.

Laliberte, A.S., and A. Rango, 2008. Incorporation of texture, intensity, hue, and saturation for rangeland monitoring with unmanned aircraft imagery, *GEOBIA 2008: Pixels, Objects, Intelligence: GEOgraphic Object Based Image Analysis for the 21st Century*, 05–08 August, Calgary, Alberta, Canada, ISPRS, Vol. No. XXXVIII-4/C1.

Laliberte, A.S., C. Winters, and A. Rango, 2008. A procedure for orthorectification of sub-decimeter resolution imagery obtained with an unmanned aerial vehicle (UAV), *Proceedings of the ASPRS 2008 Annual Convention*, 28 April - 02 May 2008, Portland, Oregon (American Society for Photogrammetry and Remote Sensing, Bethesda, Maryland), unpaginated CD-ROM.

Laliberte, A.S., and A. Rango, 2009. Texture and scale in object-based analysis of sub-decimeter resolution unmanned aerial vehicle (UAV) imagery, *IEEE Transactions on Geoscience and Remote Sensing*, 47(3):761–770.

Lambers, K., H. Eisenbeiss, M. Sauerbier, D. Kupferschmidt, T. Gaisecker, S. Sotoodeh, and T. Hanusch, 2007. Combining photogrammetry and laser scanning for the recording and modelling of the Late Intermediate Period site of Pinchango Alto, Palpa, Peru, *Journal of Archaeological Science*, 34:1702–1712.

MLB Company, 2008. MLB Company website, URL:*http://www.spyplanes.com/index.html* (last date accessed: 19 February 2010).

Nagai, M., T. Chen, R. Shibasaki, H. Kumugai, and A. Ahmed. 2009. UAV-borne 3-D mapping system by multisensory integration, *IEEE Transactions on Geoscience and Remote Sensing*, 47(3):701–708.

Patterson, M.C.L., and A. Brescia, 2008. Integrated sensor systems for UAS, *Proceedings of the 23rd Bristol International Unmanned Air Vehicle Systems (UAVS) Conference*, 07–09 April, Bristol, United Kingdom, 13 pp.

Quilter, M.C., and V.J. Anderson, 2001. A proposed method for determining shrub utilization using (LA/LS) imagery, *Journal of Range Management*, 54:378–381.

Rango, A., A.S. Laliberte, C. Steele, J.E. Herrick, B. Bestelmeyer, T. Schmugge, A. Roanhorse, and V. Jenkins, 2006. Using unmanned aerial vehicles for rangelands: Current applications and future potentials, *Environmental Practice*, 8:159–168.

Rango, A.S., A.S. Laliberte, J.E. Herrick, C. Winters, and K. Havstad, 2008. Development of an operational UAV/remote sensing capability for rangeland management, *Proceedings of the 23rd Bristol International Unmanned Air Vehicle Systems (UAVS) Conference*, 07–09 April, Bristol, United Kingdom, 9 p.

Sankey, T., C. Moffet, and K. Weber, 2008. Postfire recovery of sagebrush communities: Assessment using SPOT-5 and very large-scale aerial imagery, *Rangeland Ecology and Management*, 61:598–604.

Schaefer, R., 2004. A standards-based approach to sense-and-avoid technology, *Proceedings of the AIAA 3rd Unmanned Unlimited Technical Conference, Workshop and Exhibit*, 20–23 September, Chicago, Illinois, AIAA-2004–6420.

Yu, Q., P. Gong, N. Clinton, G. Biging, M. Kelly, and D. Schirokauer, 2006. Object-based detailed vegetation classification with airborne high spatial resolution remote sensing imagery, *Photogrammetric Engineering & Remote Sensing*, 72(7): 799–811.

Zhou, G., and D. Zang, 2007. Civil UAV system for earth observation, *Proceedings of the International Geoscience and Remote Sensing Symposium (IGARSS)*, 23–27 July, Barcelona, Spain, pp. 5319–5322.

Zhou, G.Q., 2009. Near real-time orthorectification and mosaic of small UAV video flow for time-critical event response, *IEEE Transactions on Geoscience and Remote Sensing*, 47(3):739–747.

(Received 08 April 2009; accepted 24 August 2009; final version 18 September 2009)